

Performance of 2D Photonic Crystal Fiber on Optical Waveguide Algorithm

Abstract. The photonic crystal fibers (PCFs) are designed based on optical material by periodic changes in its dielectric constant, in which a wide platform of applications in numerous domains has been provided. Many optical communication devices that are designed on the PCFs have reported high throughput in their showing, by making a significant contribution in compactness, miniature sizes and fast switching, which compose of alternate high and low refractive index materials. In this study, the PCF and the effects of translational symmetry on their properties are introduced. Two-dimensional photonic crystals (2D-PC) are studied in detail, and a new method for scattering photons off finite and infinite PCFs is developed. In this regard, the conventional fabrication methods of PCFs have been studied and a new technique for vertical etching of Polyethylene Terephthalate (PET) by ultraviolet radiation has been introduced as a powerful and economical method to implement these structures. Also, the potential of the method for fabricating higher precision and smaller dimensions has been examined. To ensure the accuracy of the proposed method, simulation was carried out using Matlab software, in which the magnitude of the light source and then the angular impact of the UV irradiation beams are investigated. In this study, the finite difference time domain (FDTD) method is accomplished for analysis of photonic-band gap (PBG) -based polarization.

Streszczenie. Światłowody fotoniczne (PCF) są projektowane w oparciu o materiał optyczny poprzez okresowe zmiany jego stałej dielektrycznej, co zapewnia szeroką platformę zastosowań w wielu dziedzinach. Wiele optycznych urządzeń komunikacyjnych zaprojektowanych na PCF odnotowało wysoką przepustowość podczas ich wyświetlania, wnosząc znaczący wkład w zwartość, miniaturowe rozmiary i szybkie przełączanie, które składają się z naprzemiennych materiałów o wysokim i niskim współczynniku załamania światła. W tym badaniu przedstawiono PCF i wpływ symetrii translacyjnej na ich właściwości. Szczegółowo badane są dwuwymiarowe kryształy fotoniczne (2D-PC) i opracowywana jest nowa metoda rozpraszania fotonów na skończonych i nieskończonych PCF. W związku z tym zbadano konwencjonalne metody wytwarzania PCF i wprowadzono nową technikę pionowego trawienia politereftalanu etylenu (PET) za pomocą promieniowania ultrafioletowego jako wydajną i ekonomiczną metodę wdrażania tych struktur. Zbadano również potencjał metody do wytwarzania wyrobów o większej precyzji i mniejszych gabarytach. Aby zapewnić dokładność proponowanej metody, przeprowadzono symulację z wykorzystaniem oprogramowania Matlab, w którym bada się wielkość źródła światła, a następnie kątowne oddziaływanie wiązek promieniowania UV. W tym badaniu metoda domeny różnic skończonych w dziedzinie czasu (FDTD) została wykorzystana do analizy polaryzacji opartej na fotonicznej przerwie wzbronionej (PBG). (Wydajność światłowodu fotonicznego 2D w algorytmie falowodu optycznego)

Keywords: Photonic Crystal Fiber (PCF), Triangular Lattice Array, Polyethylene Terephthalate (PET), FDTD method.

Słowa kluczowe: Fotoniczne włókno krystaliczne (PCF), trójkątna siatka kratowa, politereftalan etylenu (PET), metoda FDTD

Introduction

Photonic crystal fibers (PCFs) are synthetic materials, which are alternating variations of the refractive index to prevent the emission of electromagnetic waves in a range of frequencies called stopping bands. These materials are non-isotropic and heterogeneous structures with a refractive index depending on the environment changes [1-2]. Hence, these structures can be used to restrict, set up, stop, concentrate, split, disperse, and filter electromagnetic waves. The structures based on photonic band gap (PBG) have received considerable attention in recent years, so many applications are based on it [3]. The PCF has optical properties such as light concentration at a particular point, high dispersion, and anisotropy depending on specific structural parameters for instant depth of modulation that influenced refractive index, the periodic modulation, and the network type of the modulation [1,4]. In other words, considering these PCF properties, we can have more control over our designs by adjusting the parameters, which will give us more freedom to design optical instruments. The sensitivity of polarization of crystallographic photonic structures is a special property that is used to design devices with polarized sensitivity such as splitters, polarizers, and lasers [5]. The light waves in some frequency ranges are not propagated through PCFs which is called the photon's forbidden gap. The strong localization of a resonant photon is produced by impurity doping which is creating defects. This phenomenon gives complementary perfect control of light propagation and radiation by introducing line defects for PCF which resulted in a photonic crystal waveguide (PCWG) [6-7]. The PCF based on optic logic gates is deemed an important component for future research of optical devices in photonic integrated circuits.

Most of these recent applications are based on nonlinear optics, but these devices have a high power consumption and narrow operating frequency range [8]. Significant research has shown that the 2D-PC structure can utilize for optical devices and various applications such as ICs, multiplexers, wave filters, and waveguides [9-10]. In [11-12] the application of the PCWG is described as the light delivery system in heat-assisted magnetic recording (HAMR). They used a 90° bending PC-waveguide with a ridge dielectric waveguide taper coupler.

Gharaati et al. with changing elongation of the element have analyzed the change of photonic band gap (PBG) [13]. They observe that the magnitude of defect modes is not changed. Our chosen structure as you can see has TM defect mode on any angle of elongation without TE defect which is specialized in the optical polarizer. Naznin et al. simulated all-optical NOT and XOR gates that were founded by 2D-PC with a quasi-square ring cavity. The finite difference time domain (FDTD) and plane wave expansion (PWE) methods are accomplished to study crystal structure behavior. They demonstrated that for the designed structure the 180° and 90° phase differences between port signals can deliver maximum transmittance of 69% and 55% respectively [14]. Divya et al. designed an all-optical two-input NAND gate based on 2D-PC. To process the NAND gate performance, in which two resonant rings have been used, devices that are made of indium phosphide and gold rod with rectangular lattices have high-intensity optical power on PCFs based on the Kerr effect. By using PWE and FDTD methods are examined the band study and the transmittance characteristics to analyze the behavior of their choosing. They are shown consistency of simulation results with the logical table of the NAND gate by choosing

the input ports' operational wavelength at 1.55 μ m, which approves the proper quality of the device [15].

Venkatachalam et al. proposed and designed four channel 2D-PC based wavelength division demultiplexer (WDDM). The PWE and FDTD methods are utilized to estimate the photonic band gap and output spectrum of the suggested demultiplexer. They have calculated values of 93% for average transmission efficiency and an amount of 781 for the Q factor for their proposed device [16]. Fakouri-Farid et al. by using nonlinear photonic crystal ring resonators, a 1-bit optical comparator structure are proposed. These resonators are built by locating some additional dielectric rods around the core section. The rods are constructed of doped glass which has a relatively high Kerr coefficient. They applied four nonlinear resonant rings that are used with optical waveguides to make the offered comparator inside a 2D-PC structure. This structure has compared two 1-bit numbers [17]. Jayabarathan et al. have compared OR and AND logic gate functions in a triangular lattice using 2D-PC. They have analyzed some functional parameters of the logic gates by the 2D-FDTD method such as response period, contrast ratio, and bit rate. It is shown that for OR gates with two inputs, two input AND gates, and three input AND gates all parameters are desirable, and could be applied for integrated optics [18]. Shaik and Rangaswamy offer the layout of an all-optical AND gate based on 2D-PC combined with the Si rods in the air by two AND gates. One of them with and the other without probe input are suggested by structures that are designed with T-shaped waveguides without nonlinear materials employed. The configuration of the suggested AND gate structures is examined by PWE and FDTD methods. They are shown one T-shaped waveguide is required for AND gate without probe input, and two are needed with probe input. It is expressed that the small size T-shaped structures are appropriate for on-chip photonic integrated circuits design [19]. Xiaoyu et al. changed their approach by choosing long single-crystal silicon fibers, which can be obtained by employing finite element modelling [20]. A laser processing graph that is created shows a space parameter within single crystals that can be developed, by using this platform. Also is shown the laser crystallizing amorphous silicon deposited can be created of single crystal silicon core fiber inside silica narrow fibers by high-pressure chemical vapor deposition. Photosensitivity reveals a similar silicon wafer, which can create these laser processing graphs to supply a framework for creating them in other materials of technological importance [20-21].

The structure of this paper is as follows; first, an investigation of the photonic crystal waveguide is introduced and optimized. Then the numerical method and modeling are briefly explained and finally, the results of the simulation and the conclusion are presented and finalized electronically.

Finite Difference Time Domain (FDTD)

FDTD method [22], with the use of the YEE algorithm in the time-dependent discrete loop of the Maxwell equations, is used for both E and H polarization. Given the Maxwell equations, the harmonic functions E (r, t) and H (r, t) can be written as inverse Fourier transforms in time and space [23] and with respect to Bloch's theorem [24]. In solid state physics and the Brillouin zone (BZ), the main cells in the cross-lattice are obtained as follows for polarization E and H, respectively. FDTD method is a time-consuming analysis method and is the best method for analyzing PCFs. In this method, the structure is divided into a square grid and is considered a stepped approximation for environmental parameters. In discrete magnetic fields, the Maxwell

equations are replaced by differential approximation, and then the fields are calculated over time. The discrete-field components are expressed in terms of the following relation:

$$(1) \quad F^n(i, j, k) = F(\Delta x \vec{i} + \Delta y \vec{j} + \Delta z \vec{k}; n \Delta t)$$

As we see F consider one of the six components of the magnetic fields, Δx , Δy and Δz are respectively a special element size of meshes in the corresponding direction of x, y and z, and Δt is the stage of time calculation. Numerical stability and its conditions are the most important feature of any numerical method. FDTD uses a differential version, so, it is conditionally stable. The FDTD sustainability is subject to the following condition:

$$(2) \quad 0 \leq \Delta t \leq \frac{1}{c \sqrt{\frac{1}{(\Delta x)^2} + \frac{1}{(\Delta y)^2} + \frac{1}{(\Delta z)^2}}}$$

Where $c = 3 \times 10^8 \frac{m}{s}$ is known as the speed of light in a vacuum. This condition states that the defined velocity of the numerical phase should not be greater than the speed of light. But one of the drawbacks of the FDTD method is to limit the computational window. Since the numerical methods solve a finite space, the computational structure of the structure must be limited. Therefore, an unpaved PML numerical model is presented, which is the best method for limiting the computational window. Since PML is an uneven substance, the waves are expressed in terms of the following equations.

$$(3) \quad \nabla \times E = -j\omega\mu H$$

$$(4) \quad \nabla \times H = -j\omega\epsilon E$$

Regarding the properties of the PML, it is possible to apply conditions that minimize the number of reflections. According to the above, the FDTD is inherently suitable for solving the dispersion and propagation of waves in the time domain. In this method, it is possible to use modal analysis of PCFs, holes and waveguides with certain techniques.

The Photonic Band Gap (PBG)

The PCWG in this work is chosen at 1,550 nm as illustrated by Dalir et al., and this is created via a 2D lattice with a triangular array on their air holes [25]. At this specific wavelength has been obviously frequency-dependent refractive index 3.45 [26]. This layout is selected where its band gap includes a wide overlapping area than other PCF lattices and is corresponding to both transverse electric (TE) and transverse magnetic (TM) modes [23].

a. Polyethylene Terephthalate

The method used to construct 2D-PC in this paper is PET. Due to the very small dimensions and high order required for the realization of PCFs, a high degree of accuracy is required in the molding machine. For this reason, the PET polymerization technique is considered and explored in detail in this section. PET is a completely recyclable material and at the same time resistant to all materials (except for alcohol), which is why it is commonly used in the manufacture of beverage containers and other foodstuffs, synthetic fibers and other thermoforming applications. In addition, the material is lightweight and can be rigid or flexible, depending on the thickness and length and the manner in which its polymer chains can be arranged. Gas, moisture, alcohol and other solvents do not pass through and are naturally clear and colorless. PET absorbs a little bit of moisture, but if the same PET is

heated, the hydrolysis of water between the water and its molecules will change its chemical content.

The PET anisotropy etching is influenced by irradiance and UV radiation; it is a phenomenon that has been observed for the first time in the thin film lab of the University of Tehran. Isotropic and slow etching of PET in the N Dimethylformamide or DMF is highly intensified in the direction of ultraviolet irradiation, and its heterogeneous material etching is followed. The UV effect is important enough that there is almost no detachment at the points shaded by the barrier. For becoming ensure of accuracy the recent conclusion, a simple simulation was performed using Matlab software, in which the light source was expanded and therefore the effect of the UV reflection beams was taken into account. The etching rate at any point is a linear function of the intensity of the violet rays that comes with the shadow and the effective level of PET that is in contact with the DMF at that point is calculated. Unfortunately, because of the huge waste and dispersion of PET in the wavelength range of the paper, and the low difference in PET refractive index with air, comparing these findings with simulation is not possible.

b. Design Parameters

The PBG structure used in the paper is intended to design a PBG substructure consisting of a triangular lattice of cavities in silicone air with a refractive index of 3.45 with a lattice constant of $d=0.79 \mu\text{m}$, which with the radius of the cavity in the air $r/d=0.48$. These parameters are chosen to have a maximum bandwidth of the complete photonic band gap (CPBG). There is an input for a waveguide that is caused by a linear defect, which is the same as removing a row of cavities. As it is known, the PBG structure has a complete photonic band gap, and the TM and TE polarization are within the range of the wavelength $1.3842 \leq \lambda \leq 1.478$ can be guided in the structure. It's important to note that we are actually designing a new PBG polarizer, which is created by a crystallographic phototherapy heterostructure that, in such a way, is one of the isolated light (which, depending on the conditions, cannot be TM or TE) and the other isolated light passes through, so that at the output of the waveguide we have one of the isolated states that we can use this critical feature for designing a PBG polarizer, so that after entering of light to the waveguide there will be changes in the structure of the PBG represents a way for a band gap for each of its two polarities (Figure 1).

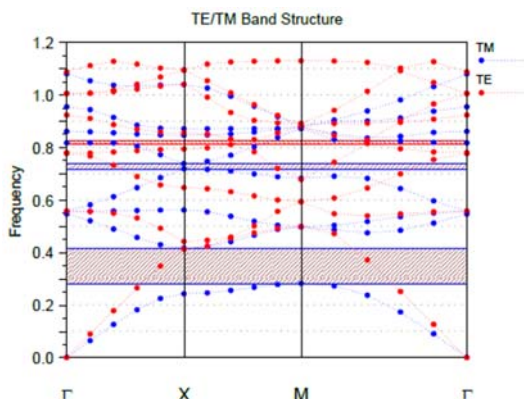


Fig. 1. The band diagram of PBG structure in Si for TE and TM modes ($r/d=0.48$)

By obtaining such a construct, a linear defect waveguide in the PCF structure is created a way by removing a number of holes, the inputs are created and then the radius of the number of holes in the air is changed, and then by removing the number of other holes we create air outlets.

Modeling of Structure

We first use the FDTD method to model the beam propagation in this waveguide. In this method, by computing the computational space and assigning the appropriate optical properties to each cell, the structure studied and the interaction fields are defined. In the FDTD method, the simulation space is divided into cubic cells and the components of the electric and magnetic fields are arranged on each cell, respectively. Then, by using the finite difference in time-dependent Maxwell equations, a set of relationships is obtained to calculate the various components of the electromagnetic field in terms of their values at the preceding time. In this algorithm, the fields are first quantified using the initial conditions and then in the time interval, the new values for each of the components are obtained by having the adjacent electric and magnetic fields at a later time step. After the simulation is completed, with the amount of electric and magnetic fields in all the cells, the desired physical quantities can be obtained. In the FDTD method, for the simulation of open-boundary problems, a fuzzy absorber layer boundary condition (PML) is used, to minimize computational space, and also by using PML to reflect electromagnetic waves into the interior. The structure prevents edges of computational space. Given the photonic crystal structure, we consider two-dimensional Maxwell equations for the transverse electric polarization state. The simulation space is also divided into square cells and time by discrete time steps. The function is then written to the grid boundaries at each time step. The 2D-FDTD time step relationships for TE mode are written as follows:

$$(5) \quad E_{x|i,j}^{n+1} = \left(\frac{\epsilon_{i,j} - \sigma_{i,j} \frac{\Delta t}{2}}{\epsilon_{i,j} + \sigma_{i,j} \frac{\Delta t}{2}} \right) E_{x|i,j}^n + \left(\frac{\Delta t}{\epsilon_{i,j} + \sigma_{i,j} \frac{\Delta t}{2}} \right) \left(\frac{H_{z|i,j+1}^n - H_{z|i,j}^n}{\Delta y} \right)$$

$$(6) \quad E_{y|i,j}^{n+1} = \left(\frac{\epsilon_{i,j} - \sigma_{i,j} \frac{\Delta t}{2}}{\epsilon_{i,j} + \sigma_{i,j} \frac{\Delta t}{2}} \right) E_{y|i,j}^n + \left(\frac{\Delta t}{\epsilon_{i,j} + \sigma_{i,j} \frac{\Delta t}{2}} \right) \left(\frac{H_{z|i+1,j}^n - H_{z|i,j}^n}{\Delta y} \right)$$

$$(7) \quad H_{z|i,j}^{n+0.5} = H_{z|i,j}^{n-0.5} - \frac{\Delta t}{\mu_{i,j}} \left(\frac{E_{y|i+1,j}^n - E_{y|i,j}^n}{\Delta x} - \frac{E_{x|i,j+1}^n - E_{x|i,j}^n}{\Delta y} \right)$$

The multiple polarity method is also used to compare modeling results. The MMP method is a semi-analytical frequency bandwidth method developed by Hafner et al. in the 1980s [27-28]. In this program, the generalized point pairing technique is used. For homogeneous domains, the computational space is divided into smaller domains. Then the electromagnetic fields in each domain are expanded with the polarities inside or outside the domain. By applying boundary conditions on boundaries between domains, the coefficients of the expansions are calculated and physical quantities can be calculated with these coefficients [27-28]. Simulations are performed for each wavelength separately.

Simulation and Results

The method which is utilized to simulate the light released to polarized PBG is provided by the FDTD

method. According to the above, the FDTD is ideally suited to solving the dispersal and propagation of waves in the time domain. In this method, it is possible to use modal analysis of PCFs, holes and waveguides with certain techniques.

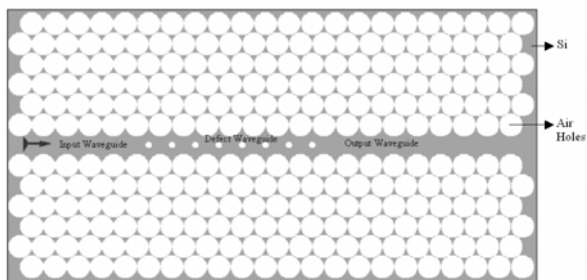


Fig. 2. Diagram of the photonic band gap polarizer

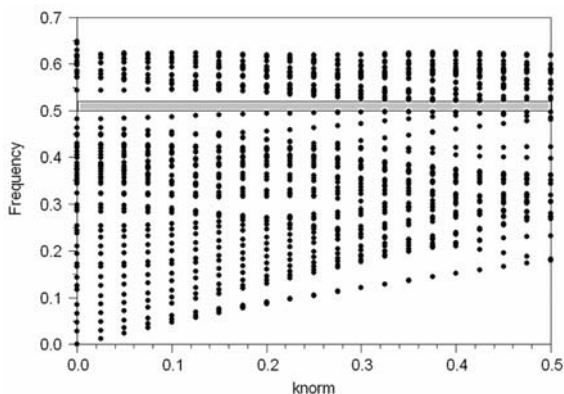


Fig. 3. Dispersion curve for waveguide linear defect for polarization TM

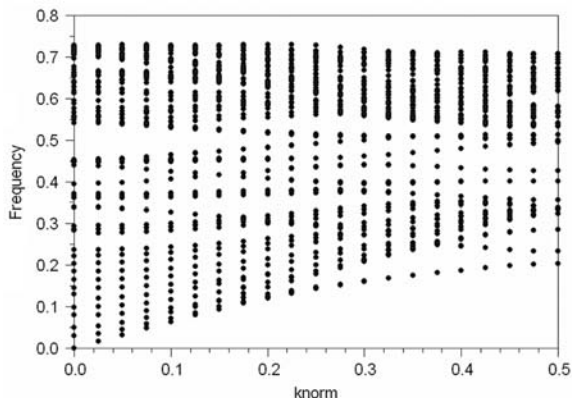


Fig. 4. Dispersion curve for waveguide linear defect for polarization TE

The air hole radii in the linear imperfection waveguide are $0.12d$. The dispersion relations for the waveguide whose defect we created for TM and TE polarization are shown in Figures 3 and 4, which show that for the PBG introduced for the TM polarization at a range of $0.3842 \leq \lambda \leq 0.5784$ while there is no such band gap for the TE polarization. The dispersion relations for the polarization of TE are shown in Figure 4. As we can see, there is a guiding mode for this structure in the region where PBG is for the polarization of TM. For simulation of the light propagation in the PBG polarizer that is illustrated, the FDTD method is performed. Figure 5 shows the images of the PBG polarizer at $\lambda = 1.55 \mu\text{m}$ for TM and TE modes respectively.

Moreover, the simulation results for wavelength $\lambda = 0.2 \mu\text{m}$ are shown for TE mode in Figure 6. It has been shown that if our incoming light is non-polarized and includes both the TE and TM polarization, in the output polarized, so that

there is a light waveguide output for the TE polarization only, there is a permissible operating area. This polarizer is located in the effective functional area $0.3842 \leq \lambda \leq 0.5784$, which produces a wide 72 nm bandwidth. This bandwidth is said to be the difference between the max and min operating wavelengths. The function of a polarizer is defined by its degree of polarization by the relation P:

$$(8) \quad P = \frac{ITE - ITM}{ITE + ITM}$$

Where ITM or ITE is the severity of the output of the TM or TE component, which is considered an effective operating area. Transmission T for a polarizer is defined as the relation 2, which is in fact a ratio of the severity of its output intensity.

$$(9) \quad T = \frac{ITE(OUT)}{ITE(IN)}$$

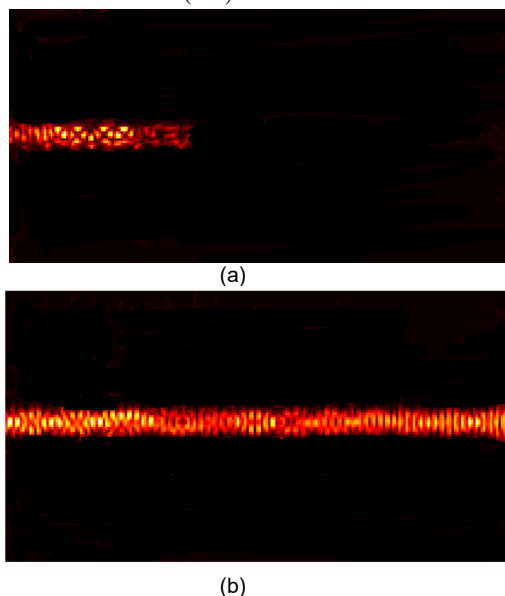
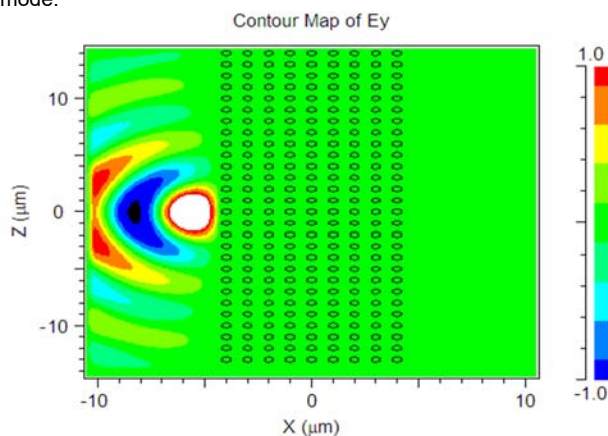


Fig. 5. Photos of the PBG polarizer at $1.55 \mu\text{m}$, (a) TM mode, (b) TE mode.



Fig/ 6. Report of a polarized PBG for polarization of TE at a wavelength $\lambda = 0.2 \mu\text{m}$.

The transmission value for the polarization TE in the target polarized is 0.5. Therefore, in Heterostructure mode, due to the changes in the radius, and finally the defect we created, we were able to create an appropriate PBG polarizer for the wavelengths in the operating range of the proposed defect bands. The PBG polarized in such a structure has advantages and disadvantages in such a way that it has a high transposition with one-side polarization but the operating limit is very narrow, so only the proper wavelengths are suitable for it.

Conclusion

In this work, PCF and the effects of translational symmetry on their properties are presented. The central part of the design of a photon crystal laser is a two-dimensional model used to limit light on the page. In a two-dimensional photonic crystal fiber model, it can be used in cross-sectional electric (TE) or magnetic (TM) modes of closed-state mode in two polarities of the classified form. In this regard, the conventional fabrication methods of PCFs have been studied and a new technique for vertical etching of Polyethylene Terephthalate (PET) by ultraviolet radiation has been introduced as a powerful and economical method to implement these structures. The PBG structure applied in the study is intended to design a PBG substructure consisting of a triangular lattice of cavities in silicone air with a refractive index and a lattice constant with the radius of the cavity. These parameters are chosen to have a maximum bandwidth of the CPBG. There is an input for a waveguide that is caused by a linear defect, which is the same as removing a row of cavities. As it is known, the PBG structure has a complete photonic band gap, and the TM and TE polarization are within the range of the wavelength $1.3842 \leq \lambda \leq 1.478$ can be guided in the structure. It's important to note that we are actually designing a new PBG polarizer, which is created by a crystallographic phototherapy heterostructure that, in such a way, is one of the isolated light and the other isolated light passes through, so that at the output of the waveguide we have one of the isolated states that we can use this critical feature to design a PBG polarizer so that after the light enters the waveguide there will be changes in the structure of the PBG in such a way that it represents a band gap for each of its two polarities. A new design of ultra-compact crystalline photonic crystal fiber PBG polarization is provided by the use of a complete photonic bands gap for TM and TE polarization. Therefore, by making the appropriate changes in the desired radius, we can create a defect and we can create an ultra-compact crystalline photonic crystal fiber PBG polarization in the appropriate wavelength range.

Authors: Mozhdeh Karamifard, Department of Physics, Aliabad Katoul Branch, Islamic Azad University, Aliabad Katoul, Iran, E-mail: mojde.karami@aliabadiu.ac.ir.

Hamed Garoosi, Ph.D. student in Electrical Engineering-Telecommunication (Wave), Babol Noshiravani University of Technology, Babol, Iran, E-mail: garoosi.hamed@gmail.com.

Seyed Mahdi Hosseini Jebelli, Department of Electrical Engineering, Technical and Vocational University (TVU), Tehran, Iran, E-mail: s.m.hosseini.jebelli@gmail.com.

REFERENCES

- [1] Villeneuve P. R. and Piche M., "Photonic band gaps in two-dimensional square and hexagonal lattices", *Phys. Rev. B*, vol. 46, (1992), pp: 4969-4972.
- [2] Sinha R.K., Kalra Y., "Design of optical waveguide polarizer using photonic band gap", *Optics express*, vol. 14, no. 22, (2006), pp: 10790-10794.
- [3] Qiu M., "Band gap effects in asymmetric photonic crystal slabs", *Physical Review B*, vol. 66, no. 3, 033103, (2002).
- [4] Karamifard M., "Assessment of Photonic Crystal Fibers for Dispersion Factor of Different Structure", *Journal of Applied Dynamic Systems and Control*, vol. 5, no. 1, (2022), pp: 21-25.
- [5] Dharchana T., Sivanantharaja A. and Selvendran S., "Design of pressure sensor using 2D photonic crystal", *Advances in Natural and Applied Sciences*, vol. 11, no. 7, (2017), pp: 26-30.
- [6] Mallika C. S., Bahaddur I., Srikanth P. C. and Sharan P., "Photonic crystal ring resonator structure for temperature measurement", *Optik*, vol. 126, no. 20, (2015), pp: 2252-2255.
- [7] Robinson S. and Nakkeeran R., "Photonic crystal ring resonator-based add drop filters: a review", *SPIE*, vol. 52, no. 6, (2013), pp: 1-15.
- [8] Tripathy S. K., Sahu S., Mohapatro C., Dash S. P., "Implementation of optical logic gates using closed packed 2D-photonic crystal structure", *Optics Communications*, vol. 285, no. 13, (2012), pp: 3234-3237.
- [9] Sreenivasulu T., Rao V., Badrinarayana T., Hegde G. K. and Srinivas T., "Photonic crystal ring resonator based force sensor: design and analysis", *Optik*, vol. 155, (2018), pp: 111-120.
- [10] Shanthy K. V. and Robinson S., "Two-dimensional photonic crystal based sensor for pressure sensing", *Photonic Sensors*, vol. 4, no. 3, (2014), pp: 248-253.
- [11] Hocini A. and Harhouz A., "Modeling and analysis of the temperature sensitivity in two dimensional photonic crystal microcavity", *Journal of Nanophotonics*, vol. 10, no. 1, (2016), pp: 016007-016010.
- [12] Radhouene M., Chhipa M. K., Najjar M., Robinson S. and Suthar B., "Novel design of ring resonator based temperature sensor using photonics technology", *Photonic Sensors*, vol. 7, no. 4, (2017), pp: 1-6.
- [13] Gharaati A. and Zahraei S. H., "Band structure engineering in 2D photonic crystal waveguide with rhombic cross-section elements", *Advances in Optical Technologies*, (2014), doi.org/10.1155/2014/780142.
- [14] Naznin S., Karim S. T., Tisa R. T. and Farhad M. A., "Design and simulation of all optical logic gates based on 2D photonic crystal fiber", *International Conference on Electrical Engineering and Information Communication Technology (ICEEICT)*, (2015), pp: 1-5. IEEE.
- [15] Divya S., Sivanantharaja A., Selvendran S., "Designing of All Optical NAND Gate Based On 2D Photonic Crystal", *Advances in Natural and Applied Sciences*, vol. 11, no. 7, (2017), pp: 36-40.
- [16] Venkatachalam K., Robinson S. and Sriram Kumar D., "Design and analysis of dual ring resonator based 2D-photonic crystal WDDM", *AIP Conference Proceedings*, vol. 1849, Iss. 1, (2017). Doi:10.1063/1.4984163.
- [17] Fakouri-Farid V., Andalib A., "Design and simulation of an all optical photonic crystal-based comparator", *Optik*, vol. 172, (2018), pp: 241-248.
- [18] Jayabarathan J. K., Subhalakshmi G., Robinson S., "Performance Evaluation of Two Dimensional Photonic Crystal Based All Optical AND/OR Logic Gates", *Journal of Optical Communications*, vol. 42, no. 3, (2018), pp: 397-407. DOI: 10.1515/joc-2018-0105.
- [19] Shaik E. H. & Rangaswamy N., "Design of photonic crystal-based all-optical AND gate using T-shaped waveguide", *Journal of Modern Optics*, vol. 63, no. 10, (2016), pp: 941-949.
- [20] Ji X., Lei S., Yu S. Y., Cheng H. Y., Liu W., Poilvert N. & Gopalan V., "Single-crystal silicon optical fiber by direct laser crystallization", *ACS Photonics*, vol. 4, no. 1, (2017), pp: 85-92.
- [21] Divya S., Sivanantharaja Avaniathan, Selvendran S., "Designing of All Optical NAND Gate Based On 2D Photonic Crystal," *Advances in Natural and Applied Sciences*, vol. 11, no. 7, (2017), pp: 36-40.
- [22] Lakshminarayanan V. & Bhattacharya I., "Advances in Optical Science and Engineering", *Springer Proceedings in Physics*, vol. 166, (2014), pp: 533-539.
- [23] Tremblay R., Doyon N. & Beaudoin-Bertrand J., "TE-TM Electromagnetic modes and states in quantum physics", (2016), arXiv preprint arXiv:1611.01472, Nov.
- [24] Vitiello M. S., Nobile M., Ronzani A., Tredicucci A., Castellano F., Talora V. & Davies A. G., "Photonic quasi-crystal terahertz lasers", *Nature Communications*, vol. 5, no. 1, (2014), pp: 1-8.
- [25] Dalir H., Xia Y., Wang Y. & Zhang X., "Athermal broadband graphene optical modulator with 35 GHz speed", *ACS photonics*, vol. 3, no. 9, (2016), pp: 1564-1568.
- [26] Arafa S., Bouchemat M., Bouchemat T., Benmerkhi A. and Hocini A., "Infiltrated photonic crystal cavity as a highly sensitive platform for glucose concentration detection", *Optics Communication*, vol. 384, (2017), pp: 93-100.
- [27] Ballisti R. & Hafner C., "The multiple multipole method in electro-and magnetostatic problems", *IEEE Transactions on Magnetism*, vol. 19, no. 6, (1983), pp: 2367-2370.
- [28] Hafner C., "The generalized multipole technique for computational electromagnetics", *Artech*, (1990). [Online Available: https://www.researchgate.net/publication/44461509_The_Generalized_Multipole_Technique_Computational_Electromagnetics]